

## Effects of Vacuum Polarization in Hadron-Hadron Scattering

D. Vetterli, W. Boeglin,<sup>(a)</sup> P. Egelhof,<sup>(b)</sup> R. Henneck, M. Jaskoła,<sup>(c)</sup> A. Klein,<sup>(d)</sup> H. Mühry,  
G. R. Plattner, and I. Sick

*Institut für Experimentelle Physik, Universität Basel, CH-4056 Basel, Switzerland*

D. Trautmann and G. Baur<sup>(e)</sup>

*Institut für Theoretische Physik, Universität Basel, CH-4056 Basel, Switzerland*

A. Weller<sup>(f)</sup>

*Max Planck Institut für Kernphysik Heidelberg, D-69 Heidelberg, Germany*

(Received 9 January 1989)

To investigate the effect of vacuum polarization in the Coulomb interaction between hadrons, the relative differential cross section for elastic  $^{12}\text{C}$ - $^{12}\text{C}$  scattering at  $E_{\text{lab}}=4$  MeV has been measured with high precision. The data are compared to theoretical calculations that take into account the contribution of the Üehling potential and other small contributions. Data and calculation agree within 1.5 standard deviations. This constitutes a test of the vacuum polarization on the 7% level.

PACS numbers: 25.70.Cd, 12.20.Fv

According to quantum electrodynamics the interaction between charges at small distances deviates from the pure Coulomb force due to vacuum polarization (VP) and further radiative corrections. Deviations of order of 1% are expected for distances which are smaller than the Compton wavelength of the electron (386 fm). Such QED effects have been investigated in a variety of systems. Whereas in leptonic systems the effect has clearly been established, and found to be in excellent agreement with QED, little information is available for the Coulomb interaction between hadrons.<sup>1-4</sup> Experiments performed using the proton-proton system<sup>1</sup> yield results which disagree with theoretical predictions by an amount that corresponds to 50% of the effect of vacuum polarization. An experiment on heavy-ion scattering,<sup>4</sup> designed for testing of the relativistic wave equation, could not detect the VP effects due to very low sensitivity of the data on the VP potential. The motivation for the present experiment is twofold: (i) to measure the contribution of vacuum polarization in a hadronic system in order to verify that the effects are the same as in leptonic systems; (ii) to test the QED predictions at shorter distances. As compared to leptonic systems heavy-ion scattering allows us to reach smaller distances.

The aim of the present experiment is to detect deviations from the cross section for scattering calculated for the pure Coulomb potential. Ideas along these lines have been pursued by several authors,<sup>5-10</sup> but the small effects expected could not experimentally be observed. To overcome these limitations, we study a system of identical particles. Mott scattering exhibits a pronounced interference structure of the angular distribution<sup>11</sup>; thus small deviations from Mott scattering are easier to detect than for the structureless angular distribution of Rutherford scattering. The ratios of cross sections measured on either side of the interference minima near  $\theta_{\text{lab}}=45^\circ$  constitute a sensitive test of the VP contribu-

tion, and are independent of the knowledge of absolute cross sections. Nevertheless, the effects are small, and the highest experimental accuracy is needed to detect the contribution due to VP. A detailed theoretical study of unwanted effects, such as nuclear interaction, nuclear polarizability, relativistic effects, and electronic screening shows that elastic scattering of  $^{12}\text{C}$  on  $^{12}\text{C}$  at  $E_{\text{c.m.}}=2$  MeV is optimal to detect VP effects in heavy-ion scattering.

The angular distribution around  $\theta_{\text{lab}}=45^\circ$  is shown in the upper part of Fig. 1. A full quantum-mechanical calculation including the Üehling potential<sup>5</sup> predicts deviations from Mott scattering of a few percent in the region where the slope of the angular distribution is largest. The expected relative changes of the cross section  $\Delta\sigma/\sigma$  are shown in the lower part of Fig. 1. The main effect of VP is a small shift in the interference minima towards  $45^\circ$ , by  $0.01^\circ$ .

The experiment, carried out at the Max Planck Institut Heidelberg, is designed to measure relative cross sections at selected angles (see Fig. 1). The setup (Fig. 2) consists of a scattering table, made of scraped bronze, housed in a scattering chamber of 1.2-m diam. The beam axis is defined by entrance and exit slits. The beam is stabilized in the  $x$  ( $y$ ) direction using the right-left (up-down) ratio of currents measured on the entrance slits. The beam divergence is minimized by placing the last quadrupole pair at a distance of 8 m from the entrance slit. The beam position and emittance is monitored continuously by two beam-scanner systems. Isotopically pure  $^{12}\text{C}$  targets of  $3 \mu\text{g}/\text{cm}^2$  thickness are used. All detectors are conventional surface-barrier detectors. The region of interest of the angular distribution ( $38^\circ < \theta_{\text{lab}} < 52^\circ$ ) is covered by a movable detector D3 which is mounted on a high-precision translation table.<sup>12</sup> The detectors D1 and D2, placed at a steep part of the angular distribution, allow a sensitive measure-

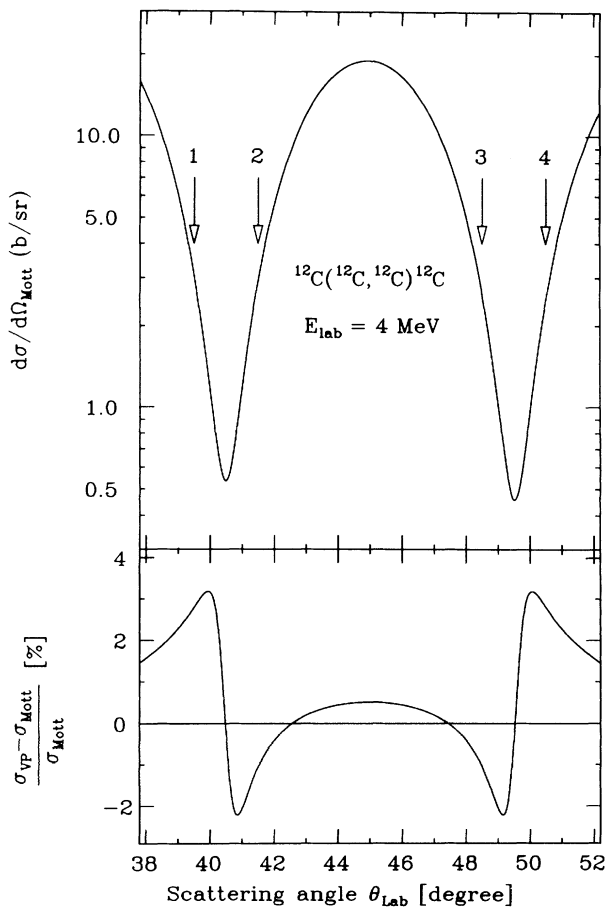


FIG. 1. Angular distribution of the differential cross section for  $^{12}\text{C}$ - $^{12}\text{C}$  Mott scattering at  $E_{\text{lab}} = 4 \text{ MeV}$  (upper part). Arrows mark the angles where data are taken ( $39.491^\circ$ ,  $41.484^\circ$ ,  $48.496^\circ$ ,  $50.489^\circ$ ). The lower part shows the relative change  $\Delta\sigma/\sigma$  of the cross sections due to the  $\ddot{\text{U}}$ ehling potential.

ment of the beam direction and its stability ( $\pm 0.001^\circ$ ). The detector D5, positioned in a maximum of the angular distribution, is used for normalization. All detectors (except D1 and D2) are working in kinematic coincidence with detectors (R3-R5) that observe the recoil particles; this allows one to eliminate background due to target impurities. A position-sensitive detector is used for R3 to, for example, separate scattering from  $^{12}\text{C}$  and  $^{13}\text{C}$ , which produces recoil nuclei that are close in angle. An identical setup (not shown in Fig. 2) is placed symmetrically to the beam, such that two independent geometries for measurements around  $\theta_{\text{lab}} = +45^\circ$  and  $-45^\circ$  are available. The positions and apertures of all collimators are measured using a precision measuring machine<sup>13</sup> that yields an accuracy of  $4 \mu\text{m}$  for all coordinates. This corresponds to an accuracy of  $0.0006^\circ$  (2 arc sec) for the angles of the various detectors. This accuracy is verified by measurements carried out at the beginning and end of the experiment.

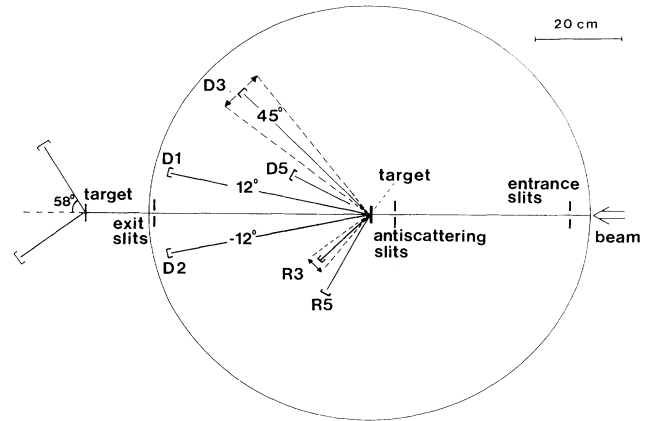


FIG. 2. Schematic view of the experimental setup.

For a precise knowledge of the effective scattering angle, the absolute target position of the thin  $^{12}\text{C}$  target (which does not necessarily coincide with the location of the target frame) and the amount of small-angle scattering in the target must be known. We obtain this information by using a coincidence distribution technique.<sup>14</sup> Two detectors at  $\pm 45^\circ$  with small  $\theta$  acceptance, one of them movable, detect scattered and recoil  $^{12}\text{C}$  ions in coincidence. From the peak position of the resulting coincidence distribution the absolute target position is deduced. Target position and target displacements (up to  $100 \mu\text{m}$ ) are measured with an accuracy of  $7 \mu\text{m}$ .<sup>14</sup> From the width and the shape of the distribution the amount of small-angle scattering in the target is determined. This yields the folding function needed for convolution of the theoretical angular distribution before comparing it with the experimental data. Small contributions of the beam divergence, detector acceptance, and size of the beam spot on the target are included automatically in this folding function. A detailed study of multiple scattering effects upon the cross section in the minimum<sup>15</sup> shows that they are understood to a degree such that they do not contribute significantly to our errors. These measurements of position and straggling are repeated for every target several times during its lifetime. The calibration of the beam energy is performed in a second small scattering chamber (see Fig. 2) using a resonance in  $^{16}\text{O}(\alpha, \alpha)^{16}\text{O}$  at  $E = 3.036 \text{ MeV}$ . The  $\alpha$  particles exciting this resonance have the same magnetic rigidity as the  $^{12}\text{C}^{2+}$  beam. The resonance energy is calibrated in a separate experiment using the Basel Cockcroft-Walton accelerator, where an analyzing magnet calibrated using many precise  $Q$  values is available. Including the error in the energy loss in the target, the effective incident energy is known to an accuracy of  $\pm 0.9 \text{ keV}$ . This accuracy is needed since the effect of a shift in energy of  $\Delta E = -20 \text{ keV}$  is similar to the one of the VP contribution.

Data are taken at four scattering angles (marked with

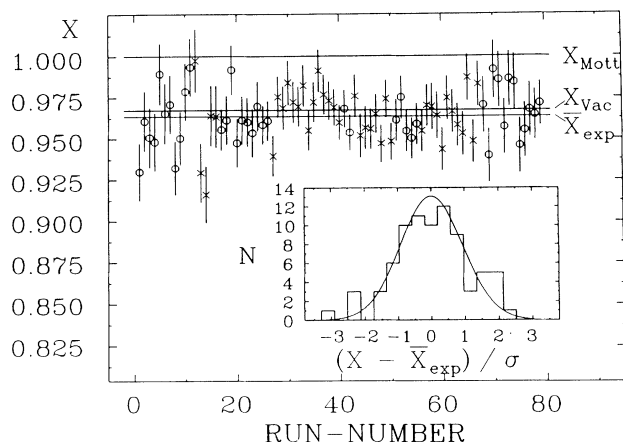


FIG. 3. Results for the average  $X$  of the ratios  $R_{12}$  and  $R_{34}$ . Each data point corresponds to one measuring cycle. The crosses (dots) mark data taken around  $\theta_{\text{lab}} = +45^\circ$  ( $-45^\circ$ ). The experimental average, the value for the pure Mott scattering, and the one for the full calculation is indicated. Inset: Plot of the distribution of measured cross-section ratios, compared to the expected Gaussian distribution.

arrows in Fig. 1). For angles 1 and 2 the influence of finite angular acceptance is almost equal, so that folding effects are eliminated in first order in the cross-section ratio  $R_{12} = \sigma(\theta_2)/\sigma(\theta_1)$ . The same holds for angles 3 and 4. In order to reduce systematic errors due to small changes of target thickness, target position, and beam alignment, many short runs are taken. Measurements within these runs are done in a sequence that eliminates all drifts of beam and target position in first order. After each cycle of cross-section measurements a set of runs is performed to measure target thickness, target position, and small-angle scattering. These calibration runs are used to correct all data.

In Fig. 3 we present the data in terms of the average  $X$  of  $R_{12}$  and  $R_{34}$ , normalized to the  $X$  value calculated for Mott scattering. This averaging suppresses in first order errors in the absolute angle calibration. Each data point represents one measuring cycle. Measurements have been performed using two fully independent detector systems around  $\theta_{\text{lab}} = +45^\circ$  (crosses) and  $-45^\circ$  (spheres)

TABLE I. Summary of the data and the theoretical prediction. The numbers given are the deviations from  $X_{\text{Mott}} = 1$  (pure Mott scattering).

Data set	$X - X_{\text{Mott}}$
Data near $\theta_{\text{lab}} = +45^\circ$	$-0.0356 \pm 0.0020$
Data near $\theta_{\text{lab}} = -45^\circ$	$-0.0374 \pm 0.0023$
Average	$-0.0364 \pm 0.0015$
Systematic errors	$\pm 0.0020$
Total error	$\pm 0.0025$
Theory (vac)	$-0.0326 \pm 0.0008$

in five separate beam times. The error bars are purely statistical and do not contain systematic errors due to the corrections applied. The distribution of all data points around the average value (marked with  $\bar{X}_{\text{exp}}$  in Fig. 3) is consistent with a statistical distribution. The  $\chi^2 \approx 1.15$  indicates that no other significant random errors are present.

Systematical errors have been carefully investigated, and their contribution to the total error is listed in Table I. The systematic error is dominated by the uncertainty in the absolute energy; multiple scattering corrections and uncertainties in the geometry of the setup give much smaller contributions. A detailed discussion of these systematic errors is found in Ref. 16.

The result of our experiment can be expressed in terms of the difference in angle of the minima at  $40^\circ$  and  $50^\circ$ . This difference is measured with an accuracy of  $0.0007^\circ$ .

For an accurate prediction of the cross section, many effects beyond first-order vacuum polarization are taken into account. Table II shows the various contributions to  $\Delta\sigma/\sigma$ . Contributions due to higher-order vacuum polarizations are calculated using potentials from Huang.<sup>17</sup> The effects of the nuclear interaction, estimated using a Woods-Saxon potential with realistic tails at large radii, are negligible because the beam energy is far below the Coulomb barrier. [The classical turning point for the system is 47 fm ( $45^\circ$ ).] For the calculation of the contribution of nuclear  $E1$  polarizability, the polarizability  $\alpha$  is taken from experimental data<sup>18</sup> on the total photon absorption cross section  $\sigma_{-2}$ . Relativistic effects are taken into account by solving the Klein-Gordon equation where reduced mass effects are calculated up to second order, thus solving the so-called Todorov equation.<sup>19</sup> For the calculation of electron screening we use a Bohr-type exponential screening function which is fitted to a realistic Hartree-Fock-Slater potential. The effective charges of projectile and target are calculated treating multiple ionization effects in the semiclassical approximation.

TABLE II. List of contributions to the deviation from Mott scattering. The numbers are normalized to the effect of first-order vacuum polarization.

Effect	Contribution (%)
Vacuum polarization of order $Z\alpha Z\alpha$ (Üehling potential)	100
Vacuum polarization of order $\alpha(Z\alpha)^2$ (Källén-Sabry)	+0.71
Vacuum polarization of order $Z\alpha(Z\alpha)^3$	-0.02
Nuclear interaction	< 0.01
Nuclear polarizability	-0.6 $\pm$ 0.1
Relativistic effects	+2.6 $\pm$ 1.0
Electronic screening	-6.6 $\pm$ 2.0
Ionization	+1.1 $\pm$ 0.5

The energy loss due to ionization during the scattering process is incorporated. A detailed account of these calculations will be published elsewhere.<sup>20</sup>

The result of these calculations shows that the first-order vacuum-polarization potential yields the largest correction to the Mott cross section. All additional effects are 1 to 2 orders of magnitude smaller.

The numerical results are summarized in Table I. The data for the two completely independent setups are in good agreement. The average agrees with the theoretical prediction within  $1.5\sigma$ . This represents a test of vacuum polarization on the 7% level.

In summary, we have performed a test of the QED vacuum polarization with hadronic probes at short distances. Such a test has become possible by exploiting the occurrence of an interference pattern in elastic scattering of identical particles. The effect of vacuum polarization has been established for the first time in a hadron-hadron scattering experiment. No evidence for a deviation from theoretical predictions is observed.

This work was supported by the Swiss National Science Foundation.

---

<sup>(a)</sup>Present address: Department of Physics, Massachusetts Institute of Technology, Cambridge, MA 02139.

<sup>(b)</sup>Present address: Gesellschaft für Schwerionenforschung, 6100-Darmstadt, Germany.

<sup>(c)</sup>Present address: Institute for Nuclear Studies, PL-00681 Warsaw, Poland.

<sup>(d)</sup>Present address: Los Alamos National Laboratory, Los Alamos, NM 87545.

<sup>(e)</sup>Present address: Institut für Kernphysik, Kernforschungsanlage Jülich, Jülich, Germany.

<sup>(f)</sup>Present address: Siemens A.G., München, Germany.

<sup>1</sup>H. Wassmer and H. Muehry, *Helv. Phys. Acta* **46**, 627 (1973).

<sup>2</sup>J. Birchall, E. Baumgartner, H. M. Friess, H. Muehry, F. Roesel, and D. Trautmann, *Helv. Phys. Acta* **50**, 509 (1977).

<sup>3</sup>Ch. Thomann, J. E. Benn, and S. Muench, *Nucl. Phys. A* **303**, 457 (1978).

<sup>4</sup>W. G. Lynch, M. B. Tsang, H. C. Bhang, J. G. Cramer, and R. J. Puigh, *Phys. Rev. Lett.* **48**, 979 (1982).

<sup>5</sup>E. A. Uehling, *Phys. Rev.* **48**, 55 (1935).

<sup>6</sup>J. Rafelski and A. Klein, *Phys. Rev. C* **9**, 1756 (1974).

<sup>7</sup>J. Rafelski and A. Klein, in *Proceedings of the International Conference on Reactions between Complex Nuclei, Nashville, Tennessee, 1974*, edited by R. L. Robinson, F. K. McGowan, J. B. Ball, and J. H. Hamilton (North-Holland, Amsterdam, 1974), p. 397.

<sup>8</sup>J. Rafelski, *Phys. Rev. C* **13**, 2086 (1976).

<sup>9</sup>R. Z. Roskies, *Phys. Rev. C* **10**, 1565 (1974).

<sup>10</sup>W. Schaefer, V. Oberacker, and G. Soff, *Nucl. Phys. A* **272**, 493 (1976).

<sup>11</sup>G. R. Platter and I. Sick, *Eur. J. Phys.* **2**, 109 (1981).

<sup>12</sup>Fabricated by *Micro Controle*, 91005 Evry, France.

<sup>13</sup>Société d'Instruments de Physique, Genève, Switzerland.

<sup>14</sup>M. Jaskola, P. Egelhof, R. Henneck, H. Muehry, I. Sick, and D. Vetterli, *Nucl. Instrum. Methods A* **273**, 441 (1988).

<sup>15</sup>M. Jud, diplomarbeit, University of Basel, 1987 (unpublished).

<sup>16</sup>D. Vetterli, thesis, University of Basel, 1988 (unpublished).

<sup>17</sup>K. N. Huang, *Phys. Rev. A* **14**, 1311 (1976).

<sup>18</sup>J. Ahrens, H. Borchert, K. H. Czock, H. B. Eppler, H. Grimm, H. Gundrum, M. Kroening, P. Riehn, G. Sita Rahm, A. Ziegler, and B. Ziegler, *Nucl. Phys. A* **251**, 479 (1975).

<sup>19</sup>H. Pilkuhn, *Z. Phys. A* **305**, 241 (1982).

<sup>20</sup>D. Trautmann and G. Baur (to be published).